EPJ Web of Conferences **233**, 05002 (2020) https://doi.org/10.1051/epjconf/202023305002
CMPNC 2019

Micromagnetic study of the vortex state in sub-micron iron discs

Ludgero Peixoto[1,*], *C.* Sousa[1], *D.* Navas[1], and *J. P.* Araújo[1]

[1]IFIMUP and DFA, Faculdade de Ciências da Universidade do Porto, Rua do Campo Alegre 1021/1055, Porto, Portugal

Abstract. Magnetic nanostructures have been widely studied due to its potential applicability into several research fields such as data storage, sensing and biomedical applications. In this work, micromagnetic simulations (mumax3) of sub-micron iron discs are performed for different normalized inter-dot distance (distance/diameter), to better understand the magnetic behaviour of these nanostructures. Two sets of samples were studied: ideal circular discs and disc-shaped nanostructures (based on images of real samples). By analyzing the nucleation and annihilation fields and the magnetic susceptibility, it was found that the (ideal) discs could be considered as isolated for inter-dot distances greater than twice the raidus of the disc ($2R$). The difference in the shape of the disc-shaped nanostructures resulted in an in-plane anisotropy, noticeable on the hysteresis loops for different directions.

1 Introduction

Magnetic nanostructures are, currently, the focus of several research fields, such as data storage, sensing and biomedicine. One subset of these nanostructures are discs that present a magnetic vortex state in remanence. These discs can be used for data storage [1] and for cancer therapy, by magneto-mechanically induced cell death [2]. The vortex state is a direct result of the geometry and aspect ratio of the nanostructure. In the case of the discs, the minimization of energy causes the spins to be in a curling state, gradually changing direction. They start starting parallel to the borders of the disc, remaining in-plane until there is a point where it is energetically favourable for the spins to point either up or downwards, forming the vortex core [3, 4]. This magnetic distribution is more favourable in materials with weak anisotropy [5].

To better understand the influence of the inter-dot distance in the vortex-state, micromagnetic simulations were carried out. These simulations were performed with MuMax3 software [6]. MuMax3 is a GPU-accelerated micromagnetic simulation program that calculates the space- and time-dependent magnetization dynamics in nano-/micro-sized ferromagnets using a finite-difference discretization. The scripting language resembles a subset of the Go programming language. A web-based HTML 5 user interface is provided, allowing the user to inspect and control the simulations from within a web browser [6].

When writting the scripts, firstly, the magnetic constants were defined. The iron magnetic saturation was defined as $M_{sat,Fe} = 1700 \times 10^3$ (A/m), the exchange stiffness $A_{ex,Fe} = 2.1 \times$

*e-mail: ludgero.peixoto@fc.up.pt

10^{-11} (J/m) and the magnetocristalline anisotropy used was $K_{c1,Fe} = 4.8E4$ (J/m^3). The easy axis orientation was also defined as $K_{c1v_{Fe}}$ =vector$(cos(45 * pi/180), 0, -sin(45 * pi/180))$ and $K_{c2v_{Fe}}$ =vector$(cos(45 * pi/180), 0, sin(45 * pi/180))$. Cell size was chosen to be 5 x 5 x 5 (nm^3), which is smaller than the Fe characteristic length $R_0=\frac{\sqrt{A}}{M_s}$ =8.5 nm [7], and the damping parameter was taken as 0.5, to ensure rapid convergence. The geometries used were either thin cylinders (circular discs) or the precise shape of the discs taking into account our SEM images, as will be shown. Usually, periodic boundary conditions were set, to better mimic the real sample.

The program starts by issuing a random magnetic state in the desired geometry and taking a snapshot of it, following up by minimizing the energy which results in the fundamental state, also recorded. After this step, the discs are submitted to a magnetic field loop that forces positive and negative saturation, recording the data in a table. At each step, an explicit Runge-Kutta method for advancing the Landau-Lifshitz equation is performed. RK45, the Dormand-Prince method, offers 5-th order convergence and a 4-th order error estimate used for adaptive time step control [6].

2 Ideal discs

For biological applications, not only has the size of the nanostructures to be well-controlled [8], but also is important to understand how they interact with each other. Keeping this in mind, comprehensive simulations were based on circular (ideal) cylinders. The objective was to better understand the interactions between discs with an ideal vortex behaviour, which can be seen in Figures 1 and 2. In these figures two hysteresis loops are shown, corresponding to discs of 300 nm and 50 nm in diameter and thickness, respectively, and with different inter-dot distance. There are two abrupt transitions in the magnetization, which correspond to the nucleation (H_n) and annihilation (H_a) of the vortex in the disc. By monitoring these characteristic fields we could infer about how the inter-dot distance influences the expected vortex behaviour.

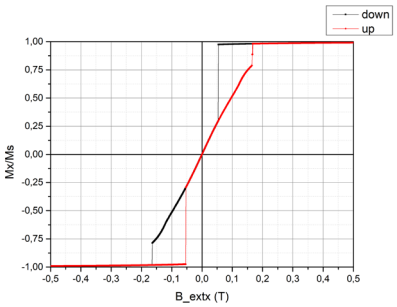

Figure 1: Hysteresis loop for a disc of 300 nm in diameter with 50 nm thickness and inter-dot distance of 35 nm.

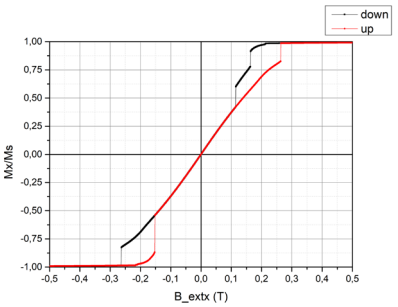

Figure 2: Hysteresis loop for a disc of 300 nm in diameter with 50 nm thickness and inter-dot distance of 300 nm.

2.1 Inter-dot interctions

For studying the inter-dot distance, in more detail, four diameters (200, 300, 400 and 500 nm) were set, for the same thickness (50 nm), varying the inter-dot distance from $R/4$ to

just above $2R$, with $24R/10$. The objective here was to assert which disc separation was the threshold to consider a disc isolated. The vortex characteristic fields' dependence with the interdot distance is presented here in Figure 3. The values for the nucleation and annihilation fields, for the same diameter, increase rapidly between $R/4$ to $4R/5$ and then starts to increase more slowly between R and $2R$, before stagnating completely, which is in agreement with a previous work for permalloy nanodiscs [9]. The behaviour can be associated to the increased magnetostatic interactions, for smaller distances, lead to the lowering of the needed field to nucleate a vortex or annihilate it [10, 11]. When the distance becomes large enough, this effect is negligible and the disc can be regarded as isolated. The described behaviour is transversal to all of the four different diameters studied. The threshold seems to be $2R$ but the difference between R and $2R$ is small enough to not be important in situations where a close-packed structure is desirable, as in magnetic memories [1, 12–14].

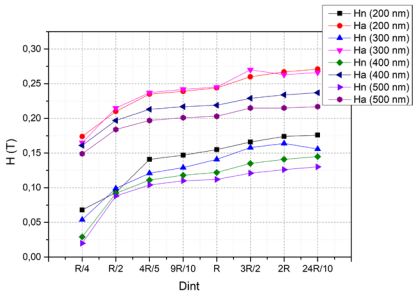

Figure 3: Nucleation (H_n) and anihilation (H_a) fields for different interdot distance (D_{int}).

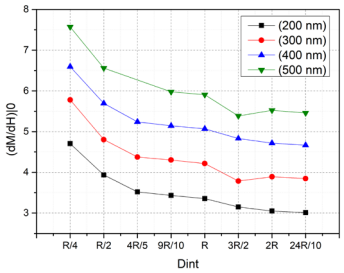

Figure 4: Magnetic susceptibility as a function of interdot distance (D_{int}).

2.2 Magnetic susceptibility

More information can be extracted from analysing the hysteresis loops, as the linear part of the loop can be associated with the vortex core motion [5]. In remanence, when the vortex is (ideally) in the centre of the disc, the moments are aligned with the borders. As the magnetic field is applied, the magnetic moments tend to align with it, disturbing the prior magnetic state and leading to a vortex core motion perpendicular to the applied field. Thus, as the magnetic susceptibility can be related with the derivative of the magnetic moment versus to the field, one can relate it to how easily a vortex core is disturbed and set in motion by an external magnetic field. The dependency on D_{int} represented in Figure 4, can be explained, once again, by the fact that being so close, the dots' magnetic moments cause their neighbours to feel higher fields than the externally applied magnetic field. With more close-packed disc arrays, this effect is accentuated, thus leading to each vortex core needing less applied field to move. As the disc separation increases, the slope value stabilizes, meaning that the disc can be considered not-affected by its neighbours, being an isolated disc [9].

3 Irregular disc-shaped nanostructures

After having dealt with ideal circular discs, the second part of this work revolved around a more practical approach, the simulation of realistically defined disc-shaped nanostructures.

Discs produced by Interference Lithography seem to be good candidates as its viewed as a low-cost technique capable of producing large areas of usable nanostructures. Basing in works using this technique [15], treated SEM images of the discs were used to define the geometry of the scripts. The idea was to replicate as accurately as possible the real sample. The intrinsic anisotropy of the disc meant it would behave differently, even depending on the direction of the in-plane applied magnetic field.

The main objective was, to study and identify typical vortex characteristics in the hysteresis loops when the applied field was parallel to the disc plane (x- and y-direction), and compare it with the ideal case, as illustrated in Figure 5. In both axes, there are two clear, abrupt, transitions corresponding to the vortex nucleation and annihilation, as well as a linear part on the hysteresis loop, representing the movement of the vortex core, as observed in the ideal dics. The vortex characteristic fields were H_n=0,0698 T, H_a=0,129 T for the x-direction and H_n=0,1129 T, H_a=0,1718 T for the y-direction. This is the first and major difference between this case and the ideal one, due to the intrinsic in-plane shape anisotropy, the characteristic fields deppend on the direction of the applied field.

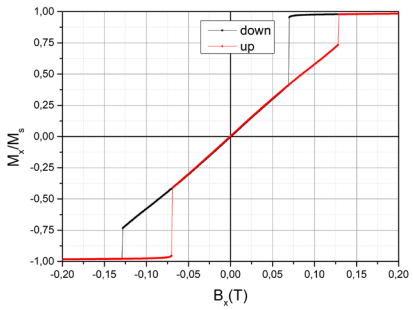

(a) Hysteresis loop in the x-direction.

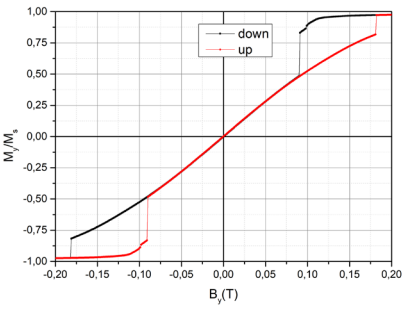

(b) Hysteresis loop in the y-direction.

Figure 5: Simulated hysteresis loop for single disc with 50 nm of Fe, for in-plane and out of plane applied magnetic field.

Figure 6 shows snapshots at six different applied fields in an array of nine discs, without periodic boundary conditions, to demonstrate the nucleation process. Starting off, all of the discs are in the saturated state (Figure 6a). As the field starts to reduce, some inhomogeneities begin to make an appearance at one of the discs in the outer rows (Figure 6b). This can be explained since no periodic boundary conditions are implemented, therefore the outer discs are the ones are less affected by their neighbours [10, 11]. Between Figure 6c and Figure 6d, all of the disc have already started to nucleate. It is noted that this transition is not as abrupt as presumed, revealing the more probabilistic nature of the event [16]. Even in Figure 6e, some inhomogeneities can be found, before the final image (Figure 6e) where the vortex is present in all of the discs and nearly centred. This images can correspond to the hysteresis loop in Figure 5a.

4 Concluding remarks

The underlying objectives of this study were to better understand the neighbouring discs' interactions and how it affects the vortex characteristic parameters (nucleation, annihilation and

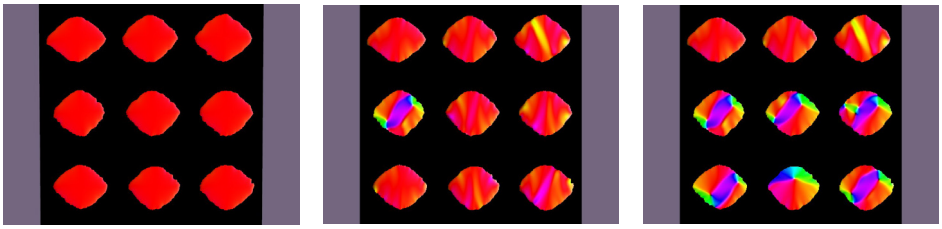

(a) B=1.0T (b) B=0.081T (c) B=0.077T

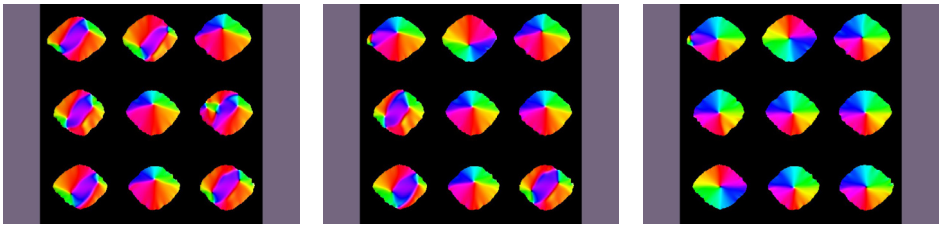

(d) B=0.067T (e) B=0.056T (f) B=0.011T

Figure 6: Field evolution of an array of 50 nm thickness Fe discs, without PBC

magnetic susceptibility). When the separation between discs was higher than 2R, the interactions were found to be negligible, and so, the disc could be considered isolated. This was consistent between all the studied parameters. Furthermore, another set of simulations were performed, based on an array of disc-shaped nanostructures with intrinsic shape anisotropy, which revealed a dependance of the charecteristic fields with the direction of the applied external field. It wasalso inferred that the discs in the extremities (with less close neighbours) were the first ones to nucleate (or annihilate) the vortex state. This difference was attributed to the smaller overal interaction of the neighbouring discs.

References

[1] S. Bohlens, B. Krüger, A. Drews, M. Bolte, G. Meier, D. Pfannkuche, Applied Physics Letters **93**, 142508 (2008), https://doi.org/10.1063/1.2998584

[2] Y. Cheng, M.E. Muroski, D.C. Petit, R. Mansell, T. Vemulkar, R.A. Morshed, Y. Han, I.V. Balyasnikova, C.M. Horbinski, X. Huang et al., Journal of Controlled Release **223**, 75 (2016), 15334406

[3] A. Wachowiak, J. Wiebe, M. Bode, O. Pietzsch, M. Morgenstern, R. Wiesendanger, Science **298**, 577 (2002)

[4] T. Shinjo, T. Okuno, R. Hassdorf, †.K. Shigeto, T. Ono, Science **289**, 930 (2000), http://science.sciencemag.org/content/289/5481/930.full.pdf

[5] K.Y. Guslienko, V. Novosad, Y. Otani, H. Shima, K. Fukamichi, Applied Physics Letters **78**, 3848 (2001)

[6] A. Vansteenkiste, J. Leliaert, M. Dvornik, M. Helsen, F. Garcia-Sanchez, B.V. Waeyenberge, AIP Advances **4**, 107133 (2014)

[7] G.S. Abo, Y.K. Hong, J. Park, J. Lee, W. Lee, B.C. Choi, IEEE Transactions on Magnetics **49**, 4937 (2013)

[8] O.V. Salata, Journal of Nanobiotechnology **2**, 1 (2004), NIHMS150003
[9] V. Novosad, K.Y. Guslienko, H. Shima, Y. Otani, S.G. Kim, K. Fukamichi, N. Kikuchi, O. Kitakami, Y. Shimada, Physical Review B **65**, 060402 (2002)
[10] K.Y. Guslienko, V. Novosad, Y. Otani, H. Shima, K. Fukamichi, Physical Review B - Condensed Matter and Materials Physics **65**, 244141 (2002)
[11] X. Zhu, V. Metlushko, B. Ilic, P. Grutter, IEEE Transactions on Magnetics **39**, 2744 (2003)
[12] N. Nishimura, T. Hirai, A. Koganei, T. Ikeda, K. Okano, Y. Sekiguchi, Y. Osada, Journal of Applied Physics **91**, 5246 (2002)
[13] R.P. Cowburn, Science **287**, 1466 (2000)
[14] J. d'Albuquerque e Castro, D. Altbir, J.C. Retamal, P. Vargas, Physical Review Letters **88**, 2372021 (2002)
[15] B. Mora, A. Perez-Valle, C. Redondo, M.D. Boyano, R. Morales, ACS Applied Materials & Interfaces **10**, 8165 (2018)
[16] A. Fernandez, C.J. Cerjan, Journal of Applied Physics **87**, 1395 (2000)